Water Practice & Technology

IWA PUBLISHING

Water Practice & Technology Vol 19 No 4, 1119 doi: 10.2166/wpt.2024.063

Remediation of toluidine blue O dye from aqueous solution using surface functionalized magnetite nanoparticles

Arti Jangra[a], Ramesh Kumar [a,*], Devender Singh[b], Harish Kumar[c], Jai Kumar[a], Parvin Kumar[a] and Suresh Kumar[a]

[a] Department of Chemistry, Kurukshetra University, Kurukshetra, Haryana 136119, India
[b] Department of Chemistry, Maharshi Dayanand University, Rohtak, Haryana 124001, India
[c] Department of Chemistry, School of Basic Sciences, Central University of Haryana, Mahendergarh 123029, India
*Corresponding author. E-mail: rameshkumarkuk@gmail.com; rameshchemkuk@kuk.ac.in

RK, 0000-0003-2089-2213

ABSTRACT

In the current study, tannic acid-functionalized iron oxide nanoparticles have been synthesized using a cost-effective co-precipitation method and subsequently characterized using various instrumentation techniques such as Fourier transform infrared spectroscopy, X-ray diffractometer, field emission scanning electron microscopy, and thermal gravimetric analysis. Further, these surface-modified magnetite nanoparticles have been used for the adsorption of toluidine dye from an aqueous solution. The adsorption process was accompanied using batch procedure, and influences of several factors such as adsorbent dose, contact time, pH, temperature, and initial concentration of adsorbate were inspected concurrently. The maximum adsorption capacity of tannic acid-functionalized magnetite nanoparticles was found to be 50.68 mg/g. The adsorption process was observed to follow the Temkin isotherm model, whereas the kinetic study was well described by pseudo-second order. The thermodynamic study revealed the adsorption process to be endothermic and spontaneous in nature with a high degree of freedom between adsorbent and adsorbate. Therefore, the study indicated that the tannic acid-functionalized magnetite nanoparticles have promising adsorption capability and can be used as an excellent adsorbent for the removal of toluidine blue O dye from the aqueous solution.

Key words: adsorption, magnetite nanoparticles, surface functionalization, tannic acid, toluidine blue O

HIGHLIGHTS

- Tannic acid-tailored magnetite nanoparticles were employed as adsorbents for the removal of coloured pollutants from an aqueous solution.
- Batch adsorption techniques were applied to scrutinize the adsorption behaviour of these magnetite nanoparticles.
- The adsorption process obeys pseudo-second-order kinetics and the Langmuir model of isotherm.
- The desorption study suggested the reusability of adsorbents.

GRAPHICAL ABSTRACT

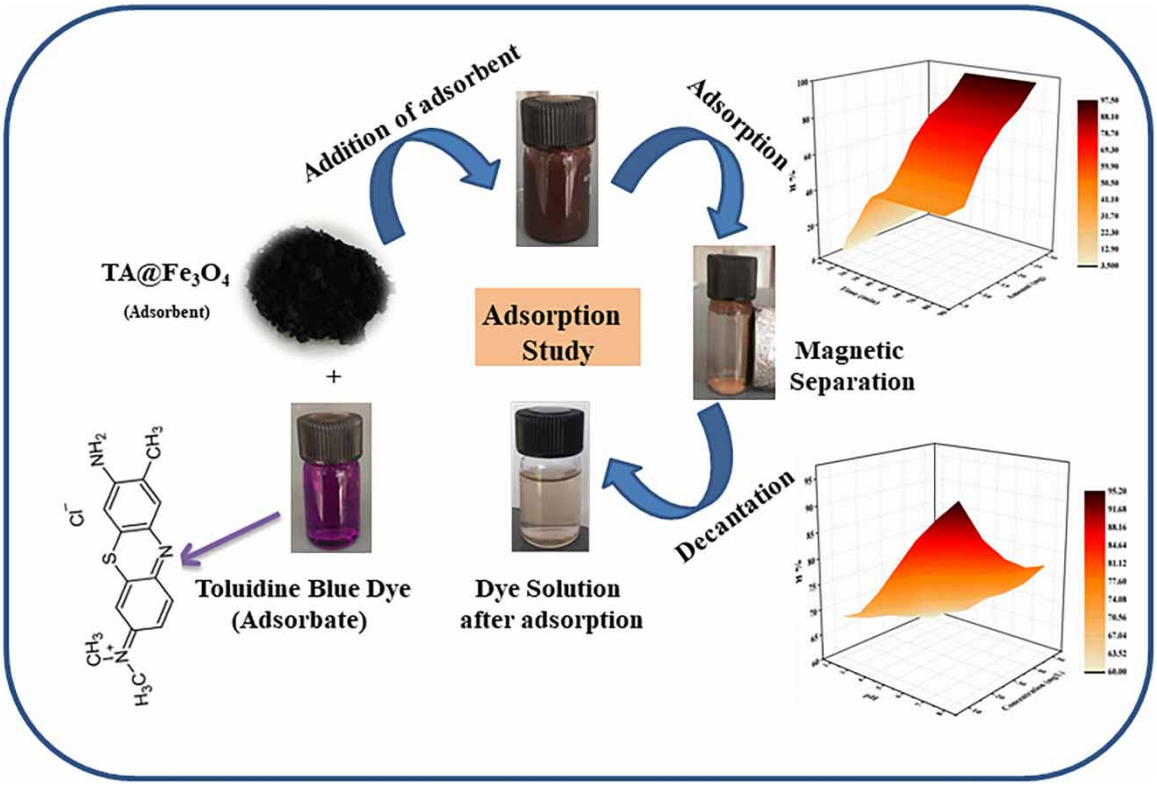

1. INTRODUCTION

Coloured effluents are major water pollutants produced by various industries including the textile industry in large quantities into nearby water sources that result in adverse effects on aquatic life and the quality of the water and thus can lead to various problems due to water toxicity. These organic substances are mainly responsible for the noxiousness and door of water. Due to their toxic effects, dye effluents are very hazardous to humans because they have both a cancer-causing and venomous perspective and could also have an effect on the direct damage of living aquatic entities (Giridhar 2014; Saura & Galindo 2016). Hence, effluents containing dye residues should be treated before they are discharged into the environment (Lairini *et al.* 2017). The basic dyes that are also termed cationic dyes including methylene blue and toluidine blue O (TBO) dye are a significant group of organic compounds and possess various scientific as well as industrial applications (Ding *et al.* 2006; Dow *et al.* 2009; Ghica & Brett 2009). Toluidine O blue dye is a basic thiazine dye, which belongs to the quinone-imine family and is selectively used in various test reactions as well as in staining acidic tissue components. In terms of wastewater purification, it is very difficult to remove cationic dye from wastewater due to its inefficient adsorption of dye effluents, high rate of redevelopment, and low frequency of flow. This issue has been considered as an attractive opportunity for researchers. In this context, various physical and chemical treatment methodology processes have been used, such as adsorption (Ferrero 2010; Islam *et al.* 2019; Dai *et al.* 2021), chemical oxidation (Türgay *et al.* 2011), electrochemical oxidation (Zhao *et al.* 2010), membrane separation (Wei *et al.* 2013), and photocatalytic oxidation (Fernandes *et al.* 2020). Of these methodologies, adsorption treatment is found to be a more efficient process for dye remediation from aqueous solutions due to its high proficiency, easy usage, and accessibility of several adsorbents. An enormous amount of synthetic as well as natural materials such as activated carbon, synthetic silica, activated aluminum oxide (Mangla *et al.* 2021), Turkish zeolite (Alpat *et al.* 2008), magnesium oxide/calcium alginate (Cui *et al.* 2021), carboxymethyl cellulose-based hydrogel (Ma *et al.* 2021), and orange peel (Lafi *et al.* 2015a; Ahmed *et al.* 2020) have been used commercially. However, such type of adsorbents are very expensive to use and show low efficacy of adsorption, less capability to separate their arduous fabrication involves high consumption of energy. To overcome these demerits, uses of new low-priced, maintainable, and advanced adsorbents are required. So, the adsorbents that

possess both properties, i.e. easy separation and good adsorption capacity, are recognized as the most effective and proficient adsorbents. Magnetic separation methodology has exponentially attracted the attention of several researchers as a fast and suitable technology for separating materials. Nowadays, magnetic nanoparticles such as magnetite (Fe_3O_4) nanoparticles have attracted the eyeballs of scientist considerably due to their special characteristics such as superparamagnetism and large surface area-to-volume ratio. Several researchers have focused on the surface modification of these magnetic nanoparticles with a suitable and appropriate material such as chitosan (Aranaz *et al.* 2019; Singh *et al.* 2021), poly-acrylic acid (Liao *et al.* 2017), aminopropyl triethoxy silane (Rajabi *et al.* 2015), multiwalled carbon nanotube (Hamidi Malayeri *et al.* 2012), and gum arabic (Kong *et al.* 2014). The surface modification helps in enhancing the stability as well as the adsorption capacities of magnetic nanoparticles. Yang *et al.* have synthesized a nanocomposite of magnetic Fe_3O_4 for the adsorption of methylene blue from aqueous solution (Yang *et al.* 2008). Rocher *et al.* developed alginate beads containing magnetic nanoparticles as well as activated carbon for the removal of organic dyes (Rocher *et al.* 2008). Adok *et al.* used surfactant-modified alumina for the removal of crystal violet from aquatic environments (Adak *et al.* 2005). Amended nanoparticles show better results, and therefore, many organic or inorganic substances have been explored to amend magnetic nanoparticles for the removal of contaminants. Tannic acid (TA) is considered humic-like substance, which can be used for the surface modification of magnetic nanoparticles, which in turn improves the properties and the adsorption capacity for the removal of dye. TA is a natural polyphenolic molecule consisting of sugar esters mainly derived from the breakdown of herbs. It has a lot of phenolic, hydroxyl, and carbonyl groups (Bagtash *et al.* 2016). Coating of TA on the surface of iron oxide nanoparticles enhances the efficiency of nanoparticles for the remediation of cationic dyes from the aqueous solution.

During the last few years, several research methods attracted the eye ball of scientists for the development of novel as well as cost-effective adsorbents. Therefore, the current study emphasizes the cheaper and easier synthesis of magnetic nanoadsorbent, i.e. TA-modified magnetite nanoparticles (TA@Fe_3O_4), for the removal of TBO dye from the aqueous solution. The physical and chemical characterizations of the synthesized TA@Fe_3O_4 nanoparticles were accompanied by analytical methods.

2. MATERIALS AND METHODS

2.1. Materials

All chemicals were of analytical reagent grade and were used without any further purification. Ferrous sulphate heptahydrate ($FeSO_4.7H_2O$), ferric chloride hexahydrate ($FeCl_3.6H_2O$), TA, and 25% ammonium hydroxide solution were purchased from SRL (India). TBO dye was used as an adsorbate throughout the experiments. Distilled water was used for the preparation of solutions.

2.2. Methods

2.2.1. Techniques used

A digital mechanical stirrer was used for the preparation of unmodified and TA-modified magnetite nanoparticles (TA@Fe_3O_4) at 2,000 rpm. The Fourier infrared spectrum of unmodified and TA-modified magnetite nanoparticles was recorded using an MB-3000 ABB FTIR spectrophotometer. Thermograms of synthesized unmodified and modified magnetic nanoparticles were obtained using a thermogravimetric (TG) analyzer, Perkin Elmer STA-6000 TG analyzer under specific conditions (5–80 °C/min heating rate and 20–1,000 °C temperature range). The point of zero charge was determined by Zeta-sizer Nano 90plus (Brookhaven Instruments Corporation). The adsorption of initial and final concentrations of dye solutions was measured by a T90 PG Instrument Limited UV-Visible spectrophotometer in the range of 190–900 nm. The size and morphology of both unmodified and TA-modified magnetic nanoparticles were investigated by Hitachi SU-8000 field emission scanning electron microscope. The X-ray diffraction patterns for synthesized magnetic nanoparticles were obtained by a diffractometer working with Cu Kα radiations of 1.540 Å wavelength over a 2θ range of 20–80°.

2.2.2. Method of preparation

The co-precipitation method was adopted as the easiest and most appropriate route way for the preparation of both unmodified and modified magnetic nanoparticles. The ferric and ferrous salts in a molar ratio of 2:1 were dissolved in 100 mL of distilled water. The aforementioned solution was stirred and heated up to 90 °C. After 10–20 min, 10 mL of ammonium hydroxide solution was added to the aforementioned solution rapidly, and the mixture was stirred for another 30 min at 90 °C. A black-coloured solution was obtained (Jangra *et al.*

2021). The solution was decanted off using a magnet, and black-coloured precipitates of unmodified magnetite nanoparticles (Fe_3O_4) were collected. To modify the surface of these synthesized magnetic nanoparticles, the solution of TA, coating material (0.5 g/20 mL), was added to the dispersed solution of unmodified magnetic nanoparticles (1.05 g Fe_3O_4 in 40 mL, sonicated for about 15 min) and stirred continuously at about 1,800–2,000 rpm for approximately 2 h (Atacan *et al.* 2016). The solution was cooled, and the black precipitates of TA@Fe_3O_4 nanoparticles were washed several times with water and separated using an external magnetic field.

2.2.3. Preparation of TBO adsorbate solution

TBO dye solution was used to prepare the stock solution (50 mg/L) by dissolving precisely amount (50 mg) of dye in deionized (1 L) and was consequently diluted to the desired concentrations. Therefore, a graph between various concentrations of TBO dye and their absorbance was plotted to obtain the calibration curve at maximum wavelength.

2.2.4. Adsorption behaviour study

The TA@Fe_3O_4 nanoparticles were used as adsorbents, and TBO dye was used as adsorbate. For this, the stock solution of TBO dye (50 mg/L concentration) was prepared and used for further process. The effect of several experimental parameters such as pH (2.0–8.0), temperature (298–323 K), adsorbent quantity (05–30 mg), and time (0–80 min) was investigated (Eleryan *et al.* 2023). The amount of known concentration of adsorbate (10 mL) was used, and the preferred pH was maintained with 0.1 M HCl or 0.1 NaOH for further studies. The values of absorbance of dye solutions before and after the treatment were measured by using a UV-visible spectrophotometer at a maximum wavelength of 630 nm using a calibration curve. To investigate the rate mechanism and nature of the adsorption process, many kinetics and isotherm models such as pseudo-first order (Langergren & Svenska 1898), pseudo-second order (Ho & McKay 1999), Langmuir (1918), Freundlich (Freundlich 1907), and Temkin (Temkin & Pyzhev 1940) were examined accordingly.

The adsorption results are represented as the value of adsorption capacity ($q_{e.\exp}$), which can be calculated as follows:

$$q_e = \frac{(C_o - C_e)V}{m} \tag{1}$$

where the percentage adsorption of the dye or dye removal efficiency can be determined using:

$$\%R = \frac{(C_o - C_e)}{C_o} \times 100 \tag{2}$$

where C_o (mg/L) is the initial concentration of dye, C_e (mg/L) is the equilibrium concentration of dye, V (L) is the volume of the solution, m (g) is the amount of adsorbent, and $q_{e.\exp}$ (mg/g) is the adsorption loading capacity.

2.2.5. Desorption study

Desorption experiments were executed to estimate the reusability of TA@Fe_3O_4 nanoparticles. Thirty milligrams of TBO dye adsorbed TA-modified magnetite (TBO@TA@Fe_3O_4) nanoparticles was stirred with 30 mL of ethanol for about 100–120 min at room temperature. After which, the magnetite nanoparticles were decanted off using a magnet and the absorbance of the decanted solution was measured at 630 nm. The desorption capacity (q_{de}) was calculated using Equation (3):

$$q_{\mathrm{de}} = \frac{C_{\mathrm{de}}V}{m} \tag{3}$$

where C_{de} (mg/L) is the concentration of dye in ethanol, V is the volume of ethanol used, and m is the mass of TBO@TA@Fe_3O_4 nanoparticles.

The percentage of desorption efficiency (W_{de}) can be expressed as follows:

$$W_{\mathrm{de}} = \frac{q_{\mathrm{e}}}{q_{\mathrm{de}}} \times 100 \tag{4}$$

After desorption, the coated nanoparticles were recollected and dried. In addition, the adsorption capacity of recycled nanoparticles was investigated again to examine the reusability.

3. RESULTS AND DISCUSSION

3.1. Characterization studies

3.1.1. Fourier transform infrared spectral studies

Infrared (IR) spectral analysis revealed the presence of functional groups in unmodified and modified magnetic nanoparticles. The spectra of unmodified, TA-modified magnetite nanoparticles and pure TA were obtained for comparative studies. The spectral peaks at low wavenumbers i.e. lower than 700 cm^{-1} were attributed to the stretching vibrations of Fe-O bonds of iron oxides. The spectra of both unmodified magnetic nanoparticles, Fe_3O_4, and TA-modified magnetic nanoparticles, TA@Fe_3O_4, depicted a strong and intense peak near 600 cm^{-1} and confirmed the presence of Fe-O bond (Figure 1). The IR spectrum of TA@Fe_3O_4 was observed to be different from that of Fe_3O_4 between 1,000 and 1,700 cm^{-1}. The broadband in the region 3,000–3,500 cm^{-1} can be assigned to the –OH stretching of the phenolic group of TA (Silverstein & Bassler 1962; Kim & Kim 2003; Özacar *et al.* 2008) and also might be attributed to the stretching of –OH bond of unmodified Fe_3O_4 nanoparticles. Two prominent peaks at 1,704 and 1,080 cm^{-1} correspond to stretching vibrations of –C = O and –C-O, respectively. Thus, the comparison of both spectra confirmed that TA is effectively coated onto the surface of unmodified magnetic nanoparticles.

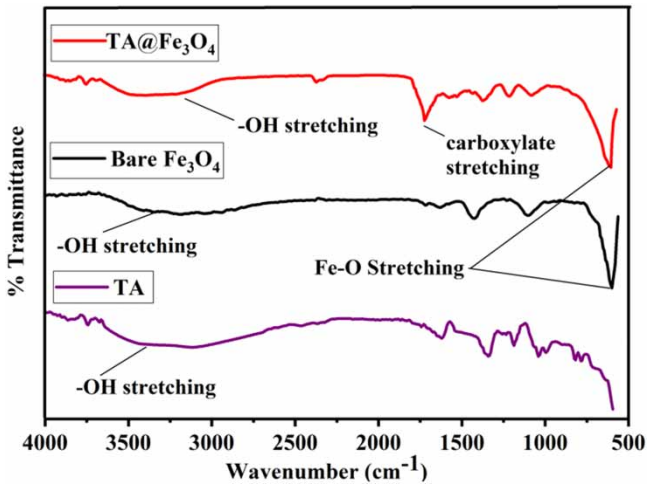

Figure 1 | FTIR spectra of bare magnetite nanoparticles (Fe_3O_4), pure tannic acid (TA), and tannic acid-coated magnetite nanoparticles (TA@Fe_3O_4).

3.1.2. X-ray diffraction studies

X-ray diffraction analysis was carried out to study the crystalline nature and the diameter of the synthesized nanoparticles, which showed a pattern having few intense peaks at 30.8°, 36°, 43.7°, 57.6°, and 63.4°. Thus, the position and intensity of these peaks suggested the semi-crystalline nature of surface-modified magnetite nanoparticles (Figure 2). The Debye–Scherrer equation was used for the calculation of the average diameter of synthesized nanoparticles.

$$d = (0.914\lambda/\beta\cos\theta)$$

whereλ is the wavelength of X-ray (1.540 A°) and β is the width of peak at half maximum θ and is Bragg angle in degree. The calculated diameter or size of synthesized TA@Fe_3O_4 nanoparticles was found to be approximately 38.5 nm.

3.1.3. Field emission electron microscopy study

Field emission electron microscopy (FESEM) studies were used to monitor the morphology as well as the size of synthesized magnetic nanoparticles. The FESEM images depicted that the average size of unmodified magnetite

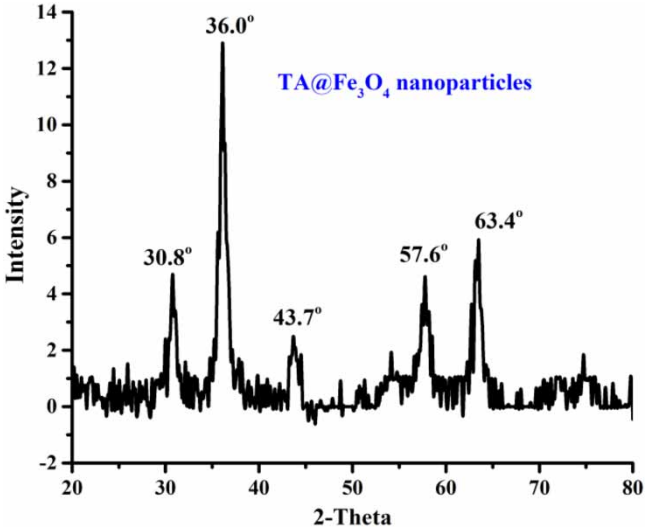

Figure 2 | X-ray diffraction pattern for tannic acid-coated magnetite nanoparticles (TA@Fe_3O_4).

(Fe_3O_4) nanoparticles and TA-modified magnetite (TA@Fe_3O_4) nanoparticles was 11 and 35 nm, respectively, which are in good agreement with the results obtained by the particle size analyzer (Figure 3). In addition, the synthesized nanoparticles were observed to have a spherical shape. The increased size of TA@Fe_3O_4 nanoparticles justified that the surface of unmodified magnetite nanoparticles (Fe_3O_4) was fruitfully modified with TA.

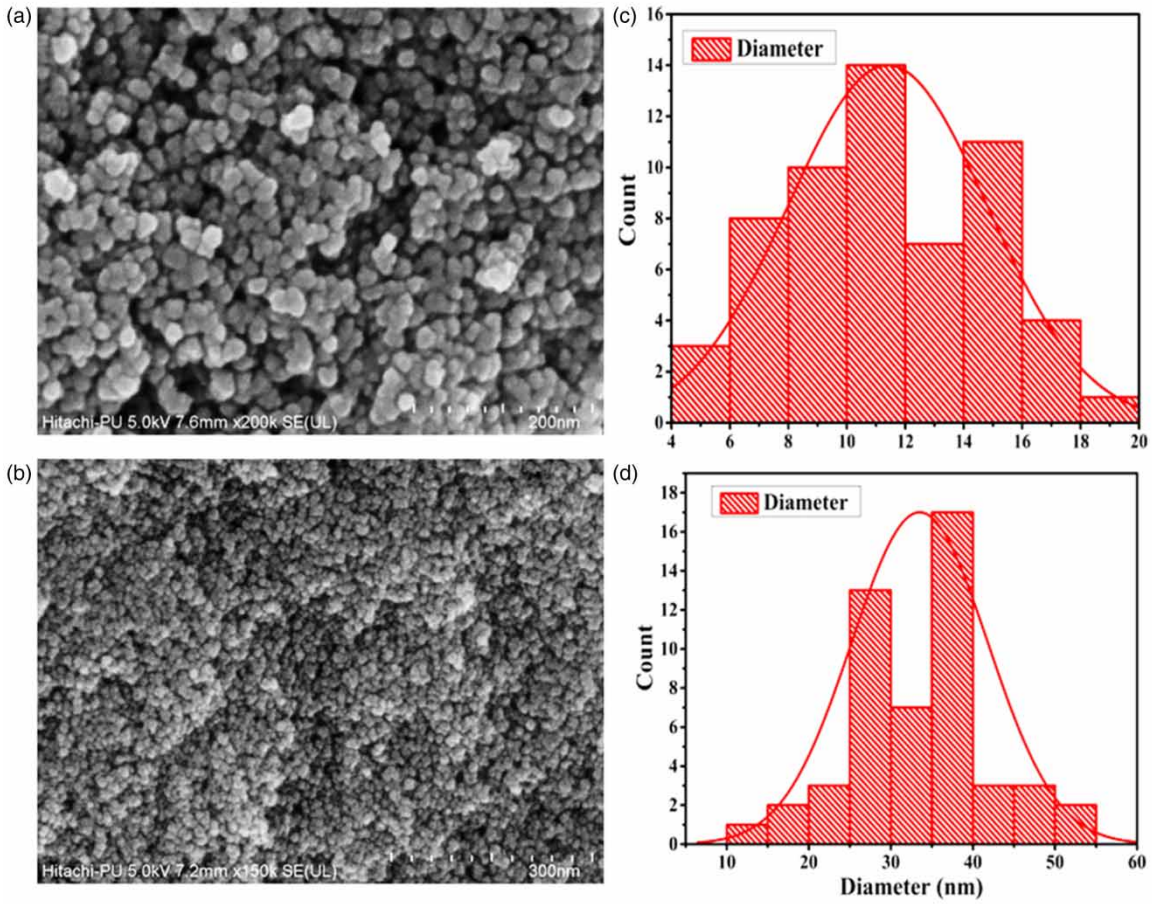

Figure 3 | FESEM images and histograms of unmodified magnetite nanoparticles ((a) and (c)) and tannic acid-modified magnetite nanoparticles ((b) and (d)).

3.1.4. TG studies

TG studies of both modified magnetite (Fe_3O_4) and TA-modified magnetite ($TA@Fe_3O_4$) nanoparticles were analysed to examine the presence of coating material, i.e. TA onto the surface of unmodified magnetite nanoparticles (Figure 4). The TG analysis displayed the different stages of weight loss for unmodified (Fe_3O_4) and surface-modified ($TA@Fe_3O_4$) magnetite nanoparticles. The weight loss (~7–10%) between 10 and 200 °C may be due to the decomposition of loosely bound water molecules. In addition, the significant weight loss of ~11.6% at the second stage (200–600 °C) may be attributed to the degradation of the organic layer, i.e. TA. Thus, the comparison of thermograms depicted that the total percentage weight loss for Fe_3O_4 and $TA@Fe_3O_4$ nanoparticles was estimated to be 11.76 and 21.6%, respectively.

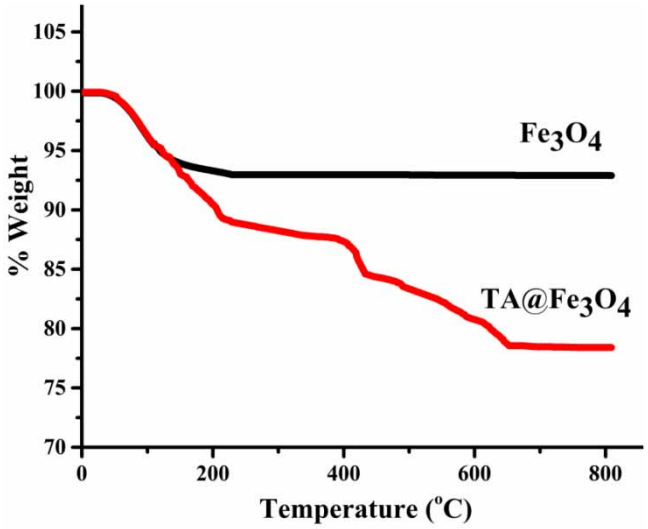

Figure 4 | Thermogravimetric curves of unmodified (Fe_3O_4) and tannic acid-modified ($TA@Fe_3O_4$) magnetite nanoparticles.

3.1.5. Zeta potential

The point of zero charge of $TA@Fe_3O_4$ nanoparticles refers to the pH of the solution at which their surface charge is equal to zero. The pH_{ZPC} of $TA@Fe_3O_4$ nanoparticles was determined by the values of zeta potential with a pH of the solution ranging from 2.0 to 8.0. The value of point of zero charge of $TA@Fe_3O_4$ nanoparticles was found at pH of ~2.0 (Figure 5). When a pH of the solution is lower than pH_{PCZ}, the surface charge of the adsorbent is positive due to the protonation of the acidic groups present in the material (Tran *et al.* 2016). When the pH of the solution is higher than the pH_{PCZ}, ionization or dissociation of the acidic oxygen surface groups occurs.

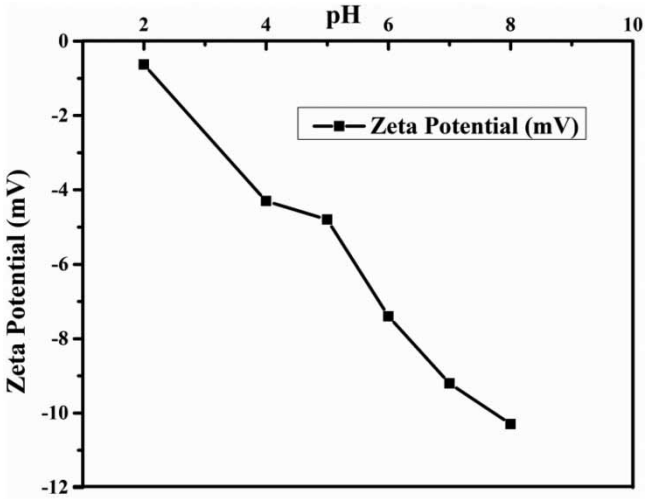

Figure 5 | Zeta potential as a function of pH of the tannic acid-modified magnetite nanoparticles ($TA@Fe_3O_4$).

3.2. Adsorption analysis

Many adsorption experiments were performed to analyse the effects of variable experimental factors including pH, temperature, adsorbent amount (TA@Fe_3O_4), adsorption time, as well as initial concentration of adsorbate on the loading capacity and removal efficiency of adsorbent, TA@Fe_3O_4.

3.2.1. Effects of solution of pH

The dye remediation efficiency of nanoparticles can be influenced by the variation of the surface charge density of surface-modified nanoparticles. The pH effect is a crucial variable for the dye removal process. The variation in pH on the removal of coloured effluents can be scrutinized in the pH range of 2.0–8.0 with a different initial concentration of adsorbate and a fixed amount of adsorbent (20 mg). The pKa value of TBO is 2.4 and 11.6 (Sabnis 2010), which suggests that the rate of degradation of the contaminant will increase in the basic medium. The point of zero charge was also found at a pH of ~2.0, which suggested that the electrostatic repulsion between sorbent and the adsorbate led to the decrease in the percentage removal efficiency of nanoparticles at low pH. The percentage of dye adsorption efficiency progressively increased with an increase in the pH of the solution ranging from 2.0 to 8.0 (Figure 6). This increasing effect may be attributed to the electrostatic interactions between the adsorbate (which possess the cationic nature) and the adsorbent. At the low value of pH, the functional groups of the adsorbate and adsorbent get protonated and both attain a positive charge and start repelling each other, which results in a decrease in the percentage removal efficiency. As the value of pH increases, the extent of protonation decreases gradually, which in turn enhances interactions between adsorbate and adsorbent molecules and permits the increase in the percentage removal efficiency. The increase in the percentage removal efficiency in the pH range from 7.0 to 8.0 may be accounted on the basis of electrostatic interactions between the negatively charged dye present on the surface of adsorbent (TA@Fe_3O_4 nanoparticles) and the positively charged TBO dye. Therefore, the study suggested that pH 8.0 is considered the optimum value of pH for better adsorption.

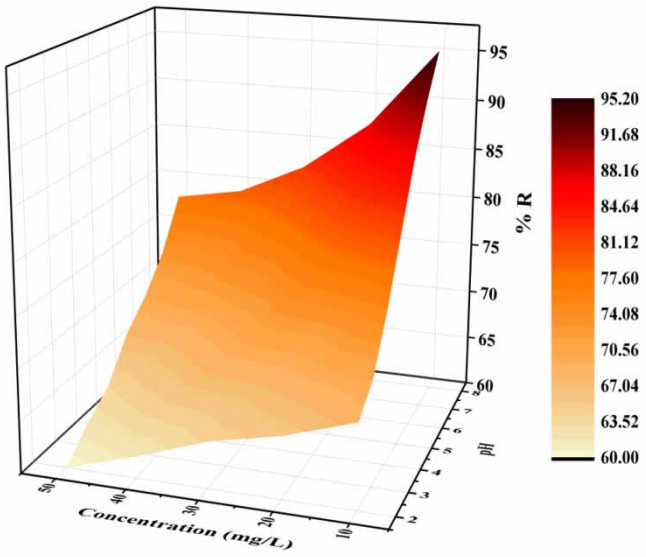

Figure 6 | Effect of pH on percentage removal of dye at different concentrations of dye solution.

3.2.2. Effect of time

The performance of synthesized adsorbent (TA-coated magnetic nanoparticles), which focused on the elimination of coloured effluents from the aqueous solution, was studied as a function of time using batch adsorption techniques at pH 8.0, a fixed concentration of adsorbate (50 mg/L), and various amounts of adsorbent (05–30 mg) at room temperature. The percentage removal efficiency of modified magnetic nanoparticles showed similar behaviour for different doses of adsorbent, which increases steadily at the initial stage with contact time and attains a state of equilibrium after 35 min (Figure 7). This behaviour of TA-modified magnetic nanoparticles can be explained on account of the fact that initially several numbers of active sites were present on the surface of synthesized TA-modified magnetite nanoparticles for the adsorption of coloured effluents. However, after a time

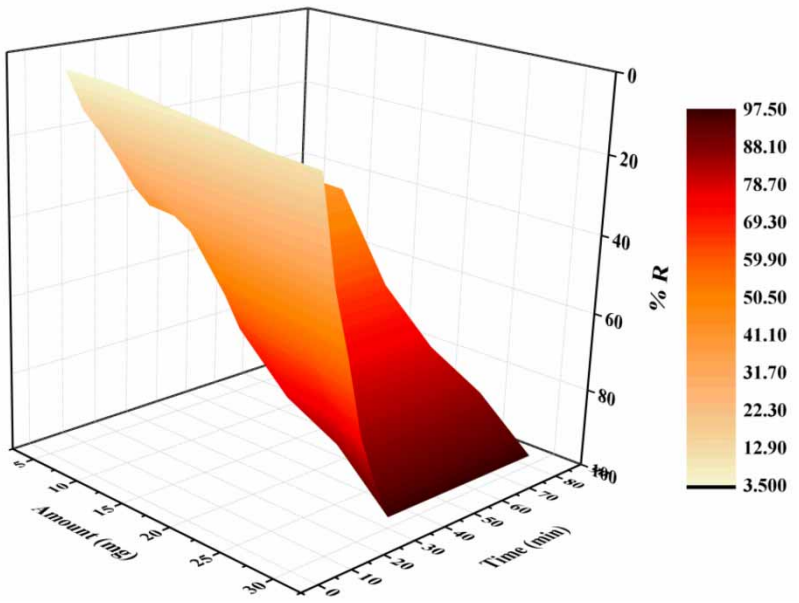

Figure 7 | Effect of contact time on percentage removal of dye for tannic acid-coated magnetite nanoparticles for different amounts of adsorbent.

lapse, the number of vacant active sites decreased, and it became a challenging process to fill these sites due to increased repulsive forces between the adsorbate and adsorbent after which no adsorption took place as equilibrium was achieved. Thus, the state of equilibrium should be treated as the optimum state for the better adsorption of TBO dye.

3.2.3. Effect of temperature

The effect of temperature on the dye elimination efficiency of nanoparticles was examined to investigate the endothermic or exothermic nature of the adsorption process. Several experiments were performed at a temperature range of 298–323 K under specific conditions using a fixed amount of adsorbent. It was noticed that the dye removal efficiency increased with the increase in temperature until the adsorption process achieved the equilibrium point, i.e. 313 K, and further a decrease was observed after 313 K (Figure 8). This decrease in the percentage of dye elimination efficiency may be attributed to the weak forces of interaction between adsorbate and adsorbent molecules (Singh *et al.* 2014) or may be due to agglomeration of nanoparticles that resulted in

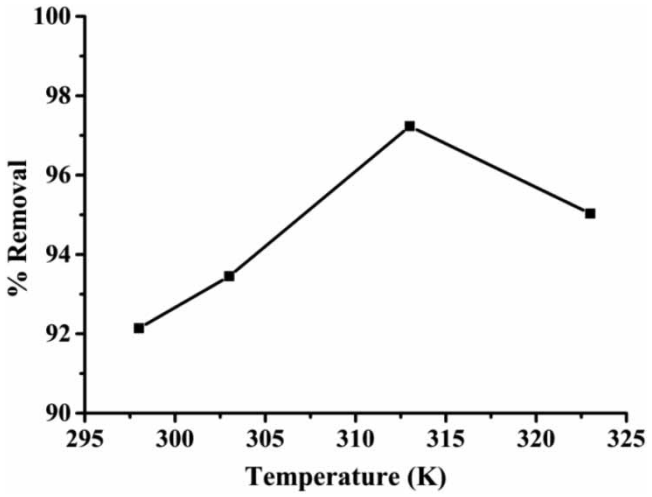

Figure 8 | Effect on temperature on the percentage removal efficiency of tannic acid-modified magnetite nanoparticles.

a decreased number of active sites for adsorption. Therefore, the temperature of 313 K was considered as the optimum value of temperature.

3.2.4. Effect of adsorbent (TA@Fe_3O_4) amount and initial concentration of adsorbate on percentage removal efficiency

The influence of the adsorbent amount on the dye elimination efficiency was examined by varying the amount of adsorbent (5–30 mg) with 10 mL of TBO dye solution of variable concentration (10–50 mg/L) under optimum conditions of pH (8.0), temperature (313 K), and time (35 min). The study revealed that the percentage of dye removal efficiency increased on increasing the amount of adsorbent and decreased on increasing the concentration of adsorbate solution (Figure 9). This increased effect can be elucidated by the fact that an increased amount of adsorbent results in more adsorption sites and a large surface area for adsorption. It was observed that a maximum of 97.23% and a minimum of 41.28% of TBO dye were removed from the aqueous solution of TBO dye (concentration 50 mg/L) for 30 and 5 mg of nanoadsorbent (TA@Fe_3O_4), respectively.

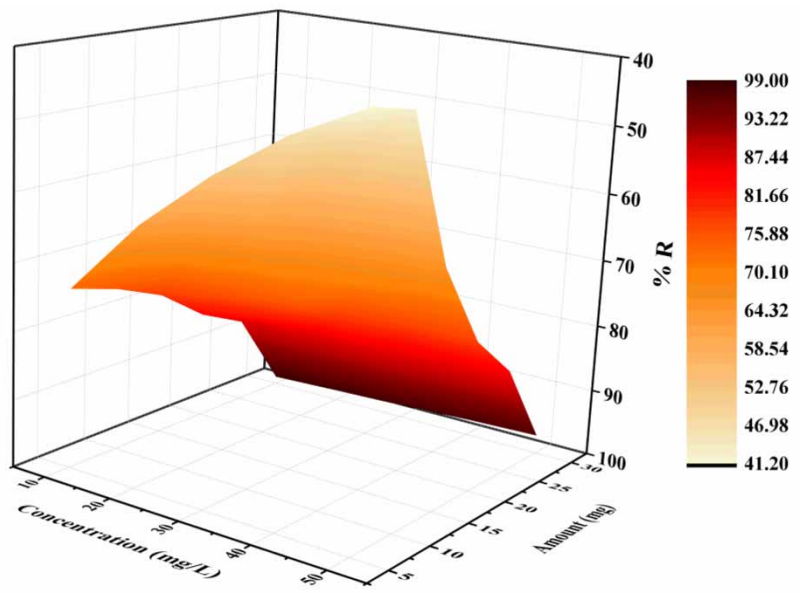

Figure 9 | Effect of adsorbent amount and initial concentration of adsorbate on percentage removal efficiency of tannic acid-modified magnetite nanoparticles.

3.2.5. Kinetic study

The kinetic study plays a key role in the determination of the rate mechanism of the adsorption process. Numerous adsorption experiments were executed at different time periods to inspect the effect of contact time using a fixed amount of adsorbent (30 mg) and a fixed concentration of dye (50 mg/L). The study led to the conclusion that the loading capacity increases rapidly at an initial stage and then starts to increase gradually till it achieves a saturation stage at 35 min. To inspect the rate of the mechanism of the adsorption process, two models of kinetics including pseudo-first-order model (Equation (5)) and pseudo-second-order model (Equation (6)) were applied simultaneously.

$$\log(q_e - q_t) = \log q_e - \frac{k_1 t}{2.303} \tag{5}$$

$$\frac{t}{q_t} = \frac{1}{k_2 q_e^2} + \frac{t}{q_e} \tag{6}$$

where q_e (mg/g) and q_t (mg/g) are the adsorption loading capacity at equilibrium and at time t (min), respectively, and k_1 (min^{-1}) and k_2 (g/mg/min) are the rate constants for pseudo-first-order and pseudo-second-order models. The value of k_1 can be obtained by plotting the graph between log ($q_e - q_t$) and time, t, whereas the value of k_2 can

be calculated from the linear plot of t/q_t versus time, t. Moreover, on comparing the kinetic variable and correlation coefficients (R^2) of both the pseudo-first-order and pseudo-second-order models, a relative kinetic study was observed to follow the pseudo-second-order model, which demonstrated the chemisorption of dyes onto the surface of nanoparticles (Figure 10).

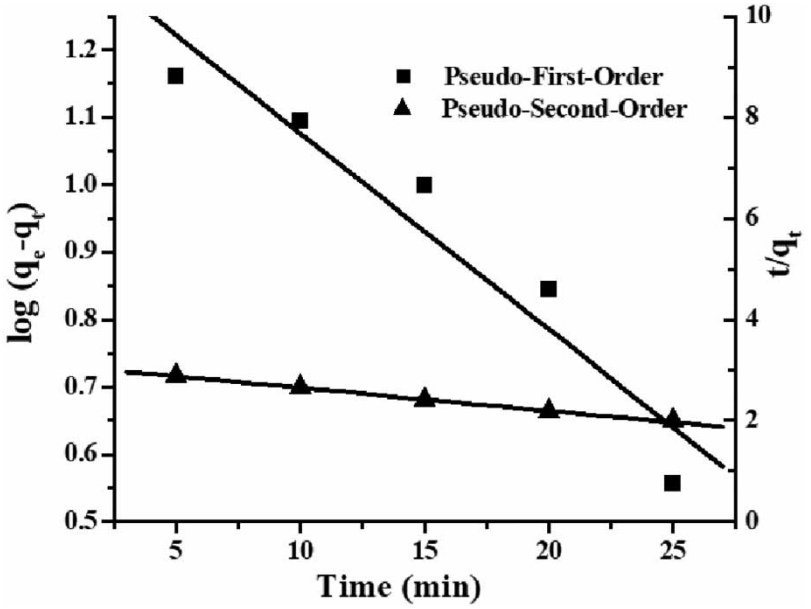

Figure 10 | Pseudo-first-order and pseudo-second-order kinetic models.

3.2.6. Adsorption isotherm analysis

The adsorption isotherm analysis is very significant to evaluate the interaction between adsorbate and adsorbent. Several isotherm models such as Langmuir (Equation (7)), Freundlich (Equation (8)), and Temkin (Equation (9)) were applied to examine the nature of the interactions among adsorbent and adsorbate. The linear forms of the isotherms were as follows:

$$\frac{C_e}{q_e} = \frac{1}{bq_m} + \frac{C_e}{q_m} \tag{7}$$

$$\log q_e = \log K_F + \frac{1}{n}\log C_e \tag{8}$$

$$q_e = B\ln A + B\ln C_e,\ B = \frac{\mathrm{RT}}{b} \tag{9}$$

where q_m (mg/g) is maximum adsorption capacity, b is the Langmuir constant, q_e (mg/g) is the loading capacity at equilibrium, K_F is the Freundlich constant, A is the Temkin constant, R is the gas constant, T (K) is the temperature, and C_e (mg/L) is the equilibrium concentration.

These isotherm analyses were performed for 10 mL of adsorbate solution of different concentrations (10–50 mg/L). A fixed amount of modified nanoparticles (5 mg) was added to the adsorbate solution, and the prepared solution was stirred for approximately 30–35 min. After that the nanoparticles were separated using an external magnetic field, and the absorbance was recorded. The measured absorbance values were used for further calculations. The isotherm curves were plotted for Langmuir, Freundlich, and Temkin to analyse the parameters. The calculated data (Table 1) suggested that the adsorption process was found to fit well with the Temkin isotherm model with a high value of coefficient of determination (0.996). Figure 11 presents the Temkin model of isotherm. The Temkin model of isotherm suggested the homogenous and multilayer adsorption of the adsorbate over the surface of the adsorbent. The maximum value of adsorption capacity was 50.68 mg/g, which was calculated from the Langmuir model for the elimination of TBO dye from the aqueous solution using TA-modified

Table 1 | Calculated values of parameters of isotherm models

Isotherm models									
Langmuir				**Freundlich**			**Temkin**		
R^2	q_m (mg/g)	K_L (L/g)	R_L	R^2	n	K_F (mg/g L/mg)	R^2	A (L/g)	B (J/mol)
0.913	50.68	0.14	0.59	0.889	2.32	2.7	0.996	0.314	11.03

Note: q_m is maximum adsorption capacity, K_L is Langmuir isotherm constant, R_L is equilibrium parameter, K_F and n are Freundlich isotherm constants, while A and B are Temkin constants.

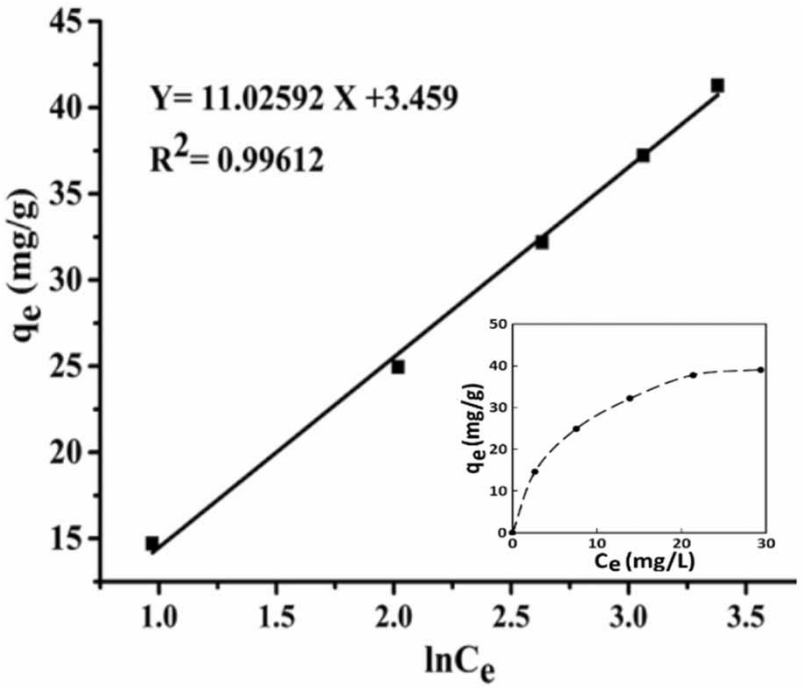

Figure 11 | Temkin isotherm model. The inset picture of C_e versus q_e plot shows the isotherm experimental data attaining the equilibrium plateau.

magnetite nanoparticles. Moreover, Equation (1) can be used for the calculation of experimental values of adsorption capacities. The experimental values of adsorption capacity for 5 mg of adsorbent are 40.28, 37.52, 32.18, 29.94, and 14.71 mg/g for variable concentrations (29.36, 21.39, 13.91, 7.53, and 2.64 mg/L, respectively).

3.2.7. Adsorption thermodynamic analysis

Adsorption thermodynamic parameters such as Gibbs free energy (ΔG), enthalpy changes (ΔH), and entropy changes (ΔS) are very helpful in the determination of favourability, spontaneity, and feasibility of the process. In the current analysis, the influence of temperature on the adsorption capacity as well as removal efficiency was used to determine the aforementioned parameters using the following equations:

$$\Delta G = -\mathrm{RT}\ln K_C \tag{10}$$

$$K_C = \frac{q_e}{C_e} \tag{11}$$

$$\Delta G = \Delta H - T\Delta S \tag{12}$$

$$\ln K_C = \frac{\Delta S}{R} - \frac{\Delta H}{\mathrm{RT}} \tag{13}$$

where R is (8.314 J/mol K) a universal gas constant, T (K) is the temperature, K_C is the distribution coefficient, and q_e (mg/g) and C_e (mg/L) are the adsorption capacity and concentration, respectively, at equilibrium point.

The values of ΔS and ΔH can be obtained from the intercept and slope of the linear graph plotted between log K_c versus $1/T$ (Figure 12). The positive value of ΔH and negative value of ΔG (Table 2) indicate the endothermic and spontaneous nature of the adsorption process, while the positive value of ΔS demonstrates the high value of degree of freedom among adsorbate and adsorbent during the adsorption process.

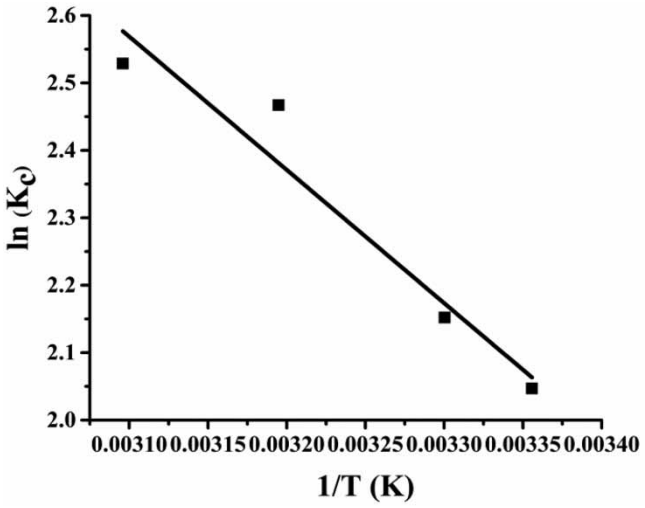

Figure 12 | Graph between ln(K_c) and $1/T$ for the calculation of thermodynamic parameters for remediation of TBO dye on tannic acid-coated magnetite nanoparticles.

Table 2 | Thermodynamic parameters for the remediation of dye on tannic acid-coated magnetite nanoparticles

Temperature (K)	lnK_c	ΔG (kJ/mol)	ΔH (kJ/mol K)	ΔS (J/mol K)
298	2.047	−5.072	16.45	72.36
303	2.152	−5.421		
313	2.467	−6.420		
323	2.528	−6.791		

Note: ΔG is change in Gibbs free energy, ΔH is enthalpy changes, ΔS is entropy changes, and K_C is distribution coefficient.

4. DESORPTION RESULTS

A desorption study was executed to inspect the adsorbent regeneration and recovery. The regeneration capacity of a biosorbent validates its applicability. The reuse of the adsorbent for TBO occurred in two cycles, using ethanol as a desorption solvent. Eighty-seven percent of desorption efficiency was obtained for the adsorbent. In addition, no significant change was observed in the adsorption capacity of recollected TA@Fe_3O_4 nanoparticles, which revealed that these modified magnetite nanoparticles can be reused for the exclusion of TBO dye from the aqueous solution.

5. COMPARISON OF PERCENTAGE REMOVAL AND MAXIMUM ADSORPTION CAPACITY OF TBO BY TA@Fe_3O_4 NANOPARTICLES WITH OTHER REPORTED ADSORBENTS

The percentage removal and maximum adsorption capacity of TBO by TA-functionalized magnetite nanoparticles were compared with already reported adsorbents (Table 3). The comparative study revealed that TA-functionalized magnetite nanoparticles are the most potential candidates among them for the removal of TBO from the aqueous solution.

6. PROPOSED ADSORPTION MECHANISM OF ADSORPTION OF TBO DYE ON THE SURFACE OF TA@Fe_3O_4 NANOPARTICLES

The adsorption of TBO dye from an aqueous solution by TA-modified magnetite nanoparticles may be explained well on the basis of different functional groups present on the surface of these nanoadsorbents. TBO may be

Table 3 | Comparison of percentage removal efficiency and maximum adsorption capacity of several adsorbents reported in literature with the present study

Sr. No.	Adsorbent used	pH	Isotherm	Kinetic order	% Removal of TBO	Adsorption capacity q_m (mg/g)	Ref
1.	Magnesium oxide	8	–	Pseudo-first order	~90	–	Mohammad Salim & Mohammad Salih (2015)
2.	Turkish zeolite	11	Langmuir and Freundlich	Pseudo-first order	–	33.03	Alpat *et al.* (2008)
3.	Fly ash	–	Freundlich	Pseudo-second order	–	6	Talman & Atun (2006)
4.	Starch sulphate	5	Toth	Pseudo-first order	–	47.13	Guo *et al.* (2011)
5.	Gypsum	6.5	Langmuir	Pseudo-second order	–	28	Rauf *et al.* (2009)
6.	Multiwalled carbon nanotubes @$NiFe_2O_4$	–	Langmuir	Pseudo-first order	65.8	25	Bahgat *et al.* (2014)
7.	Pulp fibre	6.5	Langmuir	Pseudo-second order	–	25	van de Ven *et al.* (2007)
8.	Orange peel	6	Langmuir	Pseudo-second order	72.9	–	Lafi *et al.* (2015b)
9.	TA@Fe_3O_4 nanoparticles	8	Temkin	Pseudo-second order	97.23	40.28	The present study

adsorbed onto the surface of TA-modified magnetite nanoparticles via different kinds of interactions like H-bonding, π-π interactions, and electrostatic interactions (Keshvardoostchokami *et al.* 2018). The adsorption of imidacloprid on the surface of TA-modified magnetite nanoparticles was found maximum at pH 8.0 as at this pH, hydrogen bonding and electrostatic attraction between them is maximum. From the isotherm studies, it was found that the adsorption of the adsorbate over the surface of the adsorbent was homogenous and multilayer adsorption.

7. CONCLUSION

The present study illustrated the synthesis and characterization of unmodified and TA-modified magnetite nanoparticles using several techniques such as Fourier transform infrared (FTIR) spectral study, X-ray diffraction analysis, field emission scanning electron microscopy, and TG study. In addition, numerous experiments were performed to evaluate the adsorption capacity of these nanoparticles for the degradation of TBO dye. Characterization studies suggested the successful coating of TA onto the surface of bare Fe_3O_4 nanoparticles, and FESEM images confirmed the size, 11 and 35 nm of synthesized bare Fe_3O_4 and TA@Fe_3O_4 nanoparticles, respectively. The isotherm and kinetic study depicted that the adsorption process followed the Temkin model of isotherm and pseudo-second-order kinetic with good correlation coefficients, respectively. The thermodynamic study suggested the endothermic and spontaneous nature of the adsorption process. The TA@Fe_3O_4 nanoparticles show better adsorption properties for the elimination of TBO dye. Thus, the overall study revealed that the TA@Fe_3O_4 nanoparticles can be employed as an efficient as well as eco-friendly adsorbent for the adsorption of dyes.

DATA AVAILABILITY STATEMENT

All relevant data are included in the paper or its Supplementary Information.

CONFLICT OF INTEREST

The authors declare there is no conflict.

REFERENCES

Adak, A., Bandyopadhyay, M. & Pal, A. 2005 Removal of crystal violet dye from wastewater by surfactant-modified alumina. *Separation and Purification Technology* **44**(2), 139–144.

Ahmed, M., Mashkoor, F. & Nasar, A. 2020 Development, characterization, and utilization of magnetized orange peel waste as a novel adsorbent for the confiscation of crystal violet dye from aqueous solution. *Groundwater for Sustainable Development* **10**, 100322.

Alpat, S. K., Özbayrak, Ö., Alpat, Ş. & Akçay, H. 2008 The adsorption kinetics and removal of cationic dye, toluidine blue O, from aqueous solution with Turkish zeolite. *Journal of Hazardous Materials* **151**(1), 213–220.

Aranaz, I., Alcántara, A. R., Heras, A. & Acosta, N. 2019 Efficient reduction of toluidine blue O dye using silver nanoparticles synthesized by low molecular weight chitosans. *International Journal of Biological Macromolecules* **131**, 682–690.

Atacan, K., Çakiroğlu, B. & Özacar, M. 2016 Improvement of the stability and activity of immobilized trypsin on modified Fe_3O_4 magnetic nanoparticles for hydrolysis of bovine serum albumin and its application in the bovine milk. *Food Chemistry* **212**, 460–468. Available from: https://www.sciencedirect.com/science/article/pii/S0308814616309049 (accessed 9 December 2021).

Bagtash, M., Yamini, Y., Tahmasebi, E., Zolgharnein, J. & Dalirnasab, Z. 2016 Magnetite nanoparticles coated with tannic acid as a viable sorbent for solid-phase extraction of Cd^{2+}, Co^{2+} and Cr^{3+}. *Microchimica Acta* **183**(1), 449–456. Available from: https://link.springer.com/content/pdf/10.1007/s00604-015-1667-5.pdf (accessed 9 December 2021).

Bahgat, M., Farghali, A. A., El Rouby, W. M. A. & Khedr, M. H. 2014 Efficiency, kinetics and thermodynamics of toluidine blue dye removal from aqueous solution using MWCNTs decorated with $NiFe_2O_4$. *Fullerenes Nanotubes and Carbon Nanostructures* **22**(5), 454–470.

Cui, M., Li, Y., Sun, Y., Wang, H., Li, M., Li, L. & Xu, W. 2021 Study on adsorption performance of MgO/calcium alginate composite for Congo Red in wastewater. *Journal of Polymers and the Environment* **29**(12), 3977–3987.

Dai, W., Zhang, J., Xiao, Y., Luo, W. & Yang, Z. 2021 Dual function of modified palm leaf sheath fibers in adsorbing reactive yellow 3 and Cr(VI) from dyeing wastewater. *Journal of Polymers and the Environment* **29**(12), 3854–3866.

Ding, Y., Zhang, X., Liu, X. & Guo, R. 2006 Adsorption characteristics of thionine on gold nanoparticles. *Langmuir* **22**(5), 2292–2298. Available from: https://pubs.acs.org/doi/abs/10.1021/la052897p (accessed 9 December 2021).

Dow, W. P., Li, C. C., Su, Y. C., Shen, S. P., Huang, C. C., Lee, C., Hsu, B. & Hsu, S. 2009 Microvia filling by copper electroplating using diazine black as a leveler. *Electrochimica Acta* **54**(24), 5894–5901.

Eleryan, A., Hassaan, M. A., Aigbe, U. O., Ukhurebor, K. E., Onyancha, R. B., El-Nemr, M. A., Ragab, S., Hossain, I. & El Nemr, A. 2023 Kinetic and isotherm studies of Acid Orange 7 dye absorption using sulphonated mandarin biochar treated with TETA. *Biomass Conversion and Biorefinery*. (0123456789). https://doi.org/10.1007/s13399-023-04089-w.

Fernandes, E., Contreras, S., Medina, F., Martins, R. C. & Gomes, J. 2020 N-doped titanium dioxide for mixture of parabens degradation based on ozone action and toxicity evaluation: Precursor of nitrogen and titanium effect. *Process Safety and Environmental Protection* **138**, 80–89.

Ferrero, F. 2010 Adsorption of methylene blue on magnesium silicate: Kinetics, equilibria and comparison with other adsorbents. *Journal of Environmental Sciences* **22**(3), 467–473.

Freundlich, H. 1907 Über die Adsorption in Lösungen. *Zeitschrift für Physikalische Chemie* **57U**(1), 385–470.

Ghica, M. E. & Brett, C. M. A. 2009 Poly(brilliant cresyl blue) modified glassy carbon electrodes: Electrosynthesis, characterisation and application in biosensors. *Journal of Electroanalytical Chemistry* **629**(1–2), 35–42. Available from: https://www.sciencedirect.com/science/article/pii/S0022072809000229 (accessed 9 December 2021).

Giridhar, P. 2014 A review on annatto dye extraction, analysis and processing – A food technology perspective. *Journal of Scientific Research and Reports* **3**(2), 327–348. Available from: www.sciencedomain.org (accessed 4 February 2020).

Guo, L., Li, G., Liu, J., Ma, S. & Zhang, J. 2011 Kinetic and equilibrium studies on adsorptive removal of toluidine blue by water-insoluble starch sulfate. *Journal of Chemical and Engineering Data* **56**(5), 1875–1881.

Hamidi Malayeri, F., Sohrabi, M. R. & Ghourchian, H. 2012 Magnetic multi-walled carbon nanotube as an adsorbent for toluidine blue O removal from aqueous solution. *International Journal of Nanoscience and Nanotechnology* **8**(2), 79–86. Available from: https://www.ijnnonline.net/article_3908.html (accessed 18 December 2023).

Ho, Y. S. & McKay, G. 1999 Pseudo-second order model for sorption processes. *Process Biochemistry* **34**(5), 451–465.

Islam, M. A., Ali, I., Karim, S. M. A., Hossain Firoz, M. S., Chowdhury, A. N., Morton, D. W. & Angove, M. J. 2019 Removal of dye from polluted water using novel nano manganese oxide-based materials. *Journal of Water Process Engineering* **32**, 100911.

Jangra, A., Singh, J., Khanna, R., Kumar, P., Kumar, S. & Kumar, R. 2021 Comparative studies of dye removal efficiency of surface functionalized nanoparticles with other adsorbents: Isotherm and kinetic study. *Asian Journal of Chemistry* **33**(12), 3031–3038.

Keshvardoostchokami, M., Bigverdi, P., Zamani, A., Parizanganeh, A. & Piri, F. 2018 Silver@ graphene oxide nanocomposite: Synthesize and application in removal of imidacloprid from contaminated waters. *Environmental Science and Pollution Research* **25**(7), 6751–6761.

Kim, S. & Kim, H. J. 2003 Curing behavior and viscoelastic properties of pine and wattle tannin-based adhesives studied by dynamic mechanical thermal analysis and FT-IR-ATR spectroscopy. *Journal of Adhesion Science and Technology* **17**(10), 1369–1383. Available from: http://www.tandfonline.com/doi/abs/10.1163/156856103769172797 (accessed 24 April 2020).

Kong, H., Yang, J., Zhang, Y., Fang, Y., Nishinari, K. & Phillips, G. O. 2014 Synthesis and antioxidant properties of gum arabic-stabilized selenium nanoparticles. *International Journal of Biological Macromolecules* **65**, 155–162.

Lafi, R., Rezma, S. & Hafiane, A. 2015a Removal of toluidine blue from aqueous solution using orange peel waste (OPW). *Desalination and Water Treatment* **56**(10), 2754–2765. Available from: https://www.tandfonline.com/doi/abs/10.1080/19443994.2014.982962 (accessed 18 December 2023).

Lafi, R., Rezma, S. & Hafiane, A. 2015b Removal of toluidine blue from aqueous solution using orange peel waste (OPW). *Desalination and Water Treatment* **56**(10), 2754–2765.

Lairini, S., El Mahtal, K., Miyah, Y., Tanji, K., Guissi, S., Boumchita, S. & Zerrouq, F. 2017 The adsorption of crystal violet from aqueous solution by using potato peels (Solanum tuberosum): Equilibrium and kinetic studies. *Journal of Materials and Environmental Science* **8**(9), 3252–3261.

Langergren, S. & Svenska, B. 1898 Zur theorie der sogenannten adsorption geloester stoffe.Veternskapsakad. *Handlingar* **24**, 1–39.

Langmuir, I. 1918 The adsorption of gases on plane surfaces of glass, mica and platinum. *Journal of the American Chemical Society* **40**(9), 1361–1403. Available from: https://pubs.acs.org/doi/abs/10.1021/ja02242a004 (accessed 23 January 2020).

Liao, G., Zhao, W., Li, Q., Pang, Q. & Xu, Z. 2017 Novel poly (acrylic acid)-modified tourmaline/silver composites for adsorption removal of Cu(II) ions and catalytic reduction of methylene blue in water. *Chemistry Letters* **46**(11), 1631–1634. Available from: https://www.journal.csj.jp/doi/abs/10.1246/cl.170785 (accessed 16 August 2021).

Ma, Q., Wang, W., Ge, W., Xia, L., Li, H. & Song, S. 2021 Preparation of carboxymethyl cellulose-based hydrogel supported by two-dimensional montmorillonite nanosheets for methylene blue removal. *Journal of Polymers and the Environment* **29**(12), 3918–3931.

Mangla, M., Sharma, V., Goyal, M., Chaudhary, G. R. & Sharma, M. L. 2021 Equilibrium data, kinetics and process design for the adsorptive removal of safranin-o by activated carbons. *Materials Today: Proceedings* **45**, 5479–5482. Available from: https://www.sciencedirect.com/science/article/pii/S2214785321012062 (accessed 9 December 2021).

Mohammad Salim, H. & Mohammad Salih, S. 2015 Photodegradation study of toluidine blue dye in aqueous solution using magnesium oxide as a photocatalyst. *International Journal of Chemistry* **7**(2), 143.

Özacar, M., Şengil, I. A. & Türkmenler, H. 2008 Equilibrium and kinetic data, and adsorption mechanism for adsorption of lead onto valonia tannin resin. *Chemical Engineering Journal* **143**(1–3), 32–42. Available from: https://www.sciencedirect.com/science/article/pii/S1385894707007978 (accessed 14 December 2021).

Rajabi, H. R., Arjmand, H., Hoseini, S. J. & Nasrabadi, H. 2015 Surface modified magnetic nanoparticles as efficient and green sorbents: Synthesis, characterization, and application for the removal of anionic dye. *Journal of Magnetism and Magnetic Materials* **394**, 7–13.

Rauf, M. A., Qadri, S. M., Ashraf, S. & Al-Mansoori, K. M. 2009 Adsorption studies of toluidine blue from aqueous solutions onto gypsum. *Chemical Engineering Journal* **150**(1), 90–95.

Rocher, V., Siaugue, J. M., Cabuil, V. & Bee, A. 2008 Removal of organic dyes by magnetic alginate beads. *Water Research* **42**(4–5), 1290–1298. Available from: https://www.sciencedirect.com/science/article/pii/S0043135407006252 (accessed 9 December 2021).

Sabnis, R. W. 2010 *Handbook of Biological Dyes and Stains: Synthesis and Industrial Applications*. John Wiley and Sons, Hoboken NJ.

Saura, A. V. & Galindo, F. 2016 Utilización del colorante índigo en el laboratorio docente de Química Orgánica. *Educacion Quimica* **27**(2), 133–138.

Silverstein, R. W. & Bassler, G. C. 1962 Spectrometric identification of organic compounds. *Journal of Chemical Education* **39**(11), 546–553.

Singh, D., Gautam, R. K., Kumar, R., Shukla, B. K., Shankar, V. & Krishna, V. 2014 Citric acid coated magnetic nanoparticles: Synthesis, characterization and application in removal of Cd(II) ions from aqueous solution. *Journal of Water Process Engineering* **4**(C), 233–241.

Singh, J., Jangra, A., Rani, K., Kumar, P., Kumar, S. & Kumar, R. 2021 Kinetic and thermal studies of adsorption of allura red dye by surface functionalized magnetite nanoparticles. *Asian Journal of Chemistry* **33**(11), 2675–2684.

Talman, R. Y. & Atun, G. 2006 Effects of cationic and anionic surfactants on the adsorption of toluidine blue onto fly ash. *Colloids and Surfaces A: Physicochemical and Engineering Aspects* **281**(1–3), 15–22.

Temkin, M. J. & Pyzhev, V. 1940 'Recent modifications to Langmuir isotherms, Acta Physiochim' in Ussr 12., 217.

Tran, H. N., You, S. J. & Chao, H. P. 2016 Effect of pyrolysis temperatures and times on the adsorption of cadmium onto orange peel derived biochar. *Waste Management and Research* **34**(2), 129–138.

Türgay, O., Ersöz, G., Atalay, S., Forss, J. & Welander, U. 2011 The treatment of azo dyes found in textile industry wastewater by anaerobic biological method and chemical oxidation. *Separation and Purification Technology* **79**(1), 26–33.

van de Ven, T. G. M., Saint-Cyr, K. & Allix, M. 2007 Adsorption of toluidine blue on pulp fibers. *Colloids and Surfaces A: Physicochemical and Engineering Aspects* **294**(1–3), 1–7.

Wei, X., Kong, X., Wang, S., Xiang, H., Wang, J. & Chen, J. 2013 Removal of heavy metals from electroplating wastewater by thin-film composite nanofiltration hollow-fiber membranes. *Industrial and Engineering Chemistry Research* **52**(49), 17583–17590.

Yang, N., Zhu, S., Zhang, D. & Xu, S. 2008 Synthesis and properties of magnetic Fe3O4-activated carbon nanocomposite particles for dye removal. *Materials Letters* **62**(4–5), 645–647.

Zhao, K., Zhao, G., Li, P., Gao, J., Lv, B. & Li, D. 2010 A novel method for photodegradation of high-chroma dye wastewater via electrochemical pre-oxidation. *Chemosphere* **80**(4), 410–415.

First received 4 August 2023; accepted in revised form 19 February 2024. Available online 15 March 2024